Conformation of the Hexasaccharide Repeating Subunit from the Vibrio cholerae O139 Capsular Polysaccharide †

ARTICLE *in* BIOCHEMISTRY · MAY 2003

Impact Factor: 3.02 · DOI: 10.1021/bi026700t · Source: PubMed

Conformation of the Hexasaccharide Repeating Subunit from the *Vibrio cholerae* O139 Capsular Polysaccharide†

Jacob Adeyeye,[‡,§] Hugo F. Azurmendi,[‡,||] Corne' J. M. Stroop,[‡,⊥] S. Sozhamannan,[§] A. L. Williams,[#] A. M. Adetumbi,[△] Judith A. Johnson,[§,▽,○] and C. Allen Bush*[,‡]

Department of Chemistry and Biochemistry, University of Maryland Baltimore County, Baltimore, Maryland 21250, Departments of Pathology and of Epidemiology and Preventive Medicine, University of Maryland School of Medicine, and Veterans Affairs Maryland Health Care System, Baltimore, Maryland 21202, Department of Biology, Howard University, Washington, D.C. 20059, and School of Medicine, Johns Hopkins University, Baltimore, Maryland 21205

Received August 21, 2002; Revised Manuscript Received February 5, 2003

ABSTRACT: In the past decade, several outbreaks of cholera have been reported to be caused by *Vibrio cholerae* O139, a strain which differs from the more common O1 strain in that the former is encapsulated. The hexasaccharide repeating subunit has been isolated from the *V. cholerae* O139 capsular polysaccharide by digestion with a recently discovered polysaccharide lyase derived from a bacteriophage specific for this serogroup. It specifically cleaves at a single position of the 4-linked galacturonic acid producing an unsaturated sugar product in quantities for conformational studies by ^{1}H and ^{13}C NMR spectroscopy. We report conformational studies on this oligosaccharide by molecular modeling and NMR spectroscopy including nuclear Overhauser effects and residual dipolar coupling of a sample weakly oriented in liquid crystalline solution. The structure contains a tetrasaccharide epitope homologous to the human Lewis^{b} blood group antigen, which adopts a relatively well-defined single conformation. Comparison of these results with those of a previously published study of the intact capsular polysaccharide indicates that the conformations of the epitope in the two cases are identical or at least closely similar. Thus, this epitope, which may be essential for the pathogenicity of this *V. cholerae* strain, is not a "conformational epitope" requiring a certain critical size for antigenicity as has been reported for several other bacterial capsular antigens.

Although improved sanitation in the 20th century has eliminated major outbreaks of cholera in North America, it remains a debilitating disease throughout much of the developing world with epidemics resulting in hundreds of thousands of cases and thousands of deaths in many parts of Africa, South America, and Asia. The disease is caused by *Vibrio cholerae*, a Gram-negative bacterium that is associated with brackish water. While before 1992 it was believed that cholera was caused only by serogroup O1 strains, an outbreak of disease caused by a new serogroup, O139, has spread from India and Bangladesh throughout much of Asia (*1*).

V. cholerae O139 Bengal is genetically similar to O1 El Tor strains, including the presence of cholera toxin genes, but differing in that the former has a capsular polysaccharide while the latter is not encapsulated (*2*). There is considerable evidence that the capsule is an essential virulence factor of the strain O139. Although the immunological specificity of O-serotypes in Gram-negative bacterial strains is generally assumed to arise from the polysaccharide chain of the lipopolysaccharide (LPS), strain O139 is unusual in that there is cross-reactivity between the capsule and the LPS (*3*). This phenomenon is explained by the observation that the capsule and LPS O-chain share an identical chemical structure with the LPS containing a single repeat of the subunit found in the capsule (*4*).

The structure of the capsule is unusual in that it contains a cyclic phosphate substituent on a galactopyranoside residue and its hexasaccharide repeating unit features a tetrasaccharide epitope which is homologous to the human Lewis^{b} blood group epitope. Referring to Figure 1, the 3,6-dideoxy sugar, colitose, differs from fucose only in the 3-deoxy position, with the rest of the stereochemistry of the substituents and the Galβ-(1→3)-GlcNAc being identical. The Lewis^{b} epitope lacks the cyclic phosphate. The conformation of the Lewis^{b} epitope has been studied by several research methods (*5*−*8*), showing that it adopts a relatively rigid single conformation having internal motion of the first kind. Thus, the glycosidic dihedral angles can be represented by unique values with small excursions (±15°) from that conformation. An essentially identical conformation is found for the Lewis^{b}

† Research supported by NIH Grants GM-57211 and AI-28856.

* Corresponding author. Phone: (410) 455-2506. Fax: (410) 455-2608. E-mail: bush@umbc.edu.

‡ University of Maryland Baltimore County.

§ Department of Epidemiology and Preventive Medicine, University of Maryland School of Medicine.

|| Present address: Department of Biological Chemistry, Johns Hopkins University School of Medicine, 725 N. Wolfe St., Baltimore, MD 21205.

⊥ Present address: NV Organon, P.O. Box 20, 5340 BH Oss, The Netherlands.

Howard University.

△ Johns Hopkins University.

▽ Veterans Affairs Maryland Health Care System.

○ Department of Pathology, University of Maryland School of Medicine.

10.1021/bi026700t CCC: $25.00
Published on Web 03/13/2003

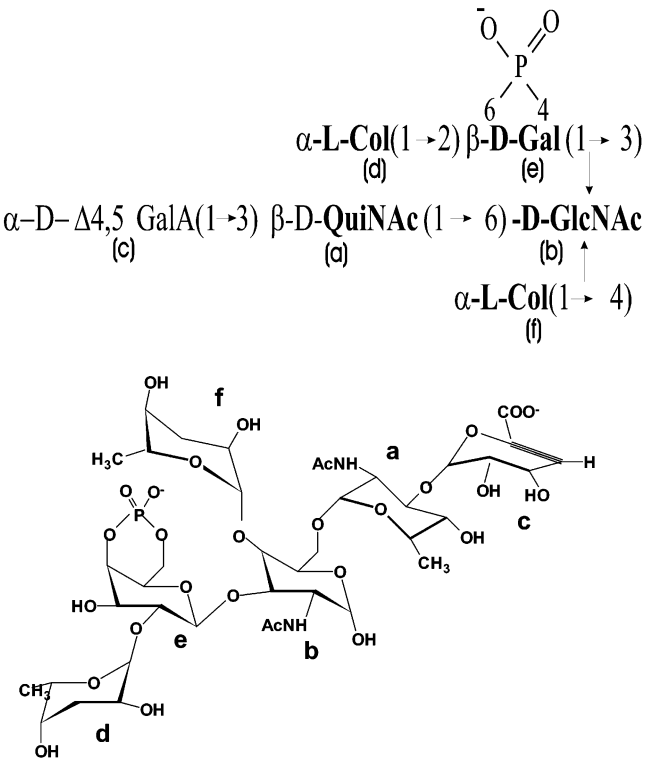

FIGURE 1: Structure of the hexasaccharide product of digestion of the capsular polysaccharide of *V. cholerae* O139 with the polysaccharide lyase.

epitope when bound to a lectin as determined by X-ray crystallography (*9*). For the case of oligosaccharides having internal motions of the second kind, which stand in contrast to relatively rigid epitopes such as the Lewis^b tetrasaccharide, wider excursions of the glycosidic dihedral angles (100−150°) occur associated with transitions between individual conformers which may be separated by energy barriers (*10*).

The conformation of the homologous tetrasaccharide epitope in the O139 capsule has been studied by ^{13}C resolved 3D NOE and molecular modeling with the conclusion that it also adopts a single rigid conformation similar to that of the Lewis^b epitope (*11*). The other two residues of the hexasaccharide subunit of the polysaccharide, galacturonic acid and *N*-acetylquinovosamine (6-deoxy-*N*-acetyl-D-glucosamine), are hypothesized to provide a flexible hinge that gives overall flexibility to this polysaccharide. The β-(1→6) linkage between residues **a** and **b** (Figure 1), having three rotatable bonds, is likely to contribute significant flexibility.

In this paper, we test whether the tetrasaccharide epitope adopts the same conformation in an isolated hexasaccharide as it does in the polymer. We report NOESY, ROESY, and RDC[1] data for a single hexasaccharide subunit. The experiments on this hexasaccharide differ from those on the polymer since its rotational correlation time, τ_c, falls in a difficult range for high-quality NOE studies. But the hexasaccharide, unlike the polymer, lends itself to study by the recently developed technique of residual dipolar coupling in weakly orienting liquid crystalline solution, and the combination of the two methods with molecular modeling is informative.

[1] Abbreviations: RDC, residual dipolar coupling; CPS, capsular polysaccharide; PFU, plaque forming units.

The comparison of the epitope conformation in the hexasaccharide and the polymer is relevant to the concept of conformational epitopes in polysaccharides (*12*). In an important series of papers, the Jennings group has shown that, for several bacterial polysaccharides having potential importance as vaccines, the conformation of the antigenically reactive epitope depends on the number of repeating units. Their proposal is supported by different antigenic reactivity of short oligosaccharides when compared to the polymer as well as by such physical measurements as NMR spectroscopy and X-ray crystallography, which have been employed to confirm this interpretation (*13*).

For the case of the *V. cholerae* O139 polysaccharide, the immunological cross-reactivity with the lipopolysaccharide, which contains a single copy of the epitope, suggests that this is not a conformational epitope (*3*). The results we report here show that the tetrasaccharide epitope in the isolated hexasaccharide is indeed very similar to that in the polymer.

For the preparation of the hexasaccharide, we have used a recently discovered lyase activity associated with a bacteriophage specific for *V. cholerae* O139 to cleave the capsule into single hexasaccharide subunits (*14*). The enzyme catalyzes a β-elimination of the 4-linked galacturonic acid in the polysaccharide backbone, producing an unsaturated sugar derivative that has also been identified as a degradation product of the lyase digestion of glycosaminoglycans such as heparin.

MATERIALS AND METHODS

Samples of the capsular polysaccharide were isolated from *V. cholerae* strain AI1837, which has been well characterized and has been shown to cause cholera in healthy North American volunteers (*15*). Single bacterial colonies grown from frozen glycerol stocks were inoculated into 10 mL of L-broth for 18 h growth at 37 °C. One milliliter of the culture was then inoculated into 1 L of L-broth and incubated overnight at 37 °C. Bacterial cells from eight 1 L batches of culture were pelleted at 10000*g* and resuspended in 120 mL of phosphate-buffered saline at pH 7.5. Capsular polysaccharide was isolated as previously described (*11*, *16*).

Bacteriophage JA-1, a gift of Dr. John Albert (*17*), was propagated on host *V. cholerae* stain AI1837 in L-broth. Then 2.5 mL of AI1837 bacterial cell suspension from an overnight culture was added to 250 mL of L-broth containing 0.2% maltose, 0.1 M $MgSO_4$, and 0.1 M $CaCl_2$. The cell culture was incubated in a gyratory shaker at 37 °C for 3 h with continuous shaking at 150 rpm before infecting it with JA-1 bacteriophage at a multiplicity of 0.1. When complete lysing of the bacteria was deemed to have occurred, based on the turbidity of the culture, 1% chloroform with 1% ethanol was added. The lysed bacterial cell debris was pelleted at 10000*g*. The supernatant was removed and centrifuged at 100000*g* for 4 h at 4 °C to recover the pelleted phages (*18*). The phages were washed twice in PBS buffer, pH 7.5, each time, recentrifuging at 100000*g* to recover the phage particles. The final pellet was dissolved in 10 mL of PBS, pH 7.5, and contained 10^{13} phages/mL as measured by a standard plaque assay.

Preliminary studies of the depolymerization of the capsule were carried out by incubating 10 mg/mL capsular polysaccharide with 10^9 PFU of bacteriophage in 1 mL of PBS buffer

at 37 °C for 3 days. Phage particles were pelleted at 100000*g*, and the supernatant was analyzed by standard SDS−PAGE/western blot (*18*) and by NMR spectroscopy to assay for the presence of oligosaccharides. SDS−PAGE gel electrophoresis was performed by the method of Laemmli (*18*). Approximately 20 μg of depolymerized capsular polysaccharide per well was separated on Novex discontinuous 4−20% precast SDS/Tris−glycine gels (Invitrogen, Carlsbad, CA) at 60 V for 1 h. For western blots, the separated capsular fragments on the SDS gel were transferred to PVDF immobilon membrane filter paper (Invitrogen) using Tris−glycine transfer buffer with 100 mA current. Blots were blocked in Tris−NaCl buffer, pH 7.5, containing 3% nonfat milk and incubated for 1 h in 1:2500 rabbit antiserum specific for AI1837 previously generated in our laboratory (*19*). The blots were washed four times each for 10 min with Tris−NaCl buffer, pH 7.5, and incubated with alkaline phosphatase-conjugated goat anti-rabbit immunoglobin G (Sigma Chemical Co.) at 1:2500 in Tris−NaCl buffer containing 3% nonfat milk for 1 h. The blot was washed four times each for 10 min in Tris−NaCl buffer and developed with Color fast detection BCIP/NBT (Sigma, St. Louis, MO).

In establishing conditions for optimum depolymerization, incubations were carried out at 37 °C in which the pH was varied in the range of 5−9 with fixed amounts of phage particles. In one study, the effect of Ca^{2+} was observed by adding 1 or 5 mM $CaCl_2$ in the presence and absence of 5 mM EDTA. In another study, the bacteriophage concentration was varied from 10^6 PFU/mL to 10^{10} PFU at fixed concentration of CPS. The extent of capsule depolymerization was followed over time by measuring UV absorbance at 232 nm, and final products were analyzed by ^{1}H NMR spectroscopy.

For a large batch preparation, 30 vials, each containing 1.2 mg of CPS and 10^{10} PFU phages in 1 mL of PBS solution, pH 7.5, with 1 mM $CaCl_2$, were incubated at 37 °C for 16 h. The phage particles were pelleted in the ultracentrifuge, and the supernatant containing 36 mg of degraded CPS was freeze-dried.

The products of bacteriophage digestion were desalted using HiTrap desalting columns (Pharmacia) eluted with 5 mM NH_4HCO_3. Oligosaccharides were detected as a void-volume peak by UV monitoring of the effluent at 205 nm. Its purity and hexasaccharide content were checked by ^{1}H NMR spectroscopy. The substantial presence of dodecasaccharide, and possibly larger fragments, prompted a gel filtration step on Bio-Gel P-6 (Bio-Rad, 45 × 1 cm) to separate hexasaccharide from larger fragments. This was performed with 5 mM NH_4HCO_3 as eluent at a flow rate of about 20 mL/h. The effluent was monitored by UV. The hexasaccharide fractions were pooled, freeze-dried, and combined.

NMR samples were exchanged three times in D_2O (99.9 atom % ^{2}H, Isotec Inc.) with intermediate lyophilization and then dissolved in D_2O (99.96 atom % ^{2}H, Isotec Inc.). NMR spectra were recorded on a 500 MHz Bruker Avance-500 spectrometer with a Bruker 5 mm broad-band triple-resonance probe. Experimental data were processed on a Silicon Graphics workstation using Felix 98.0 software (Molecular Simulations Inc.). The observed chemical shifts at 27 °C, expressed in parts per million, are reported relative to internal acetone (^{1}H, 2.225 ppm; ^{13}C, 31.07 ppm). The 1D and 2D NMR spectra of the oligosaccharide fractions were collected at 27 °C, except for the NOESY spectra, which were recorded at 15 °C. The 2D NMR spectra of hexasaccharide samples in liquid crystal media were recorded at 20 °C for the isotropic phase and at 35 °C for the anisotropic phase. One-bond ^{13}C−^{1}H couplings were measured both by ^{13}C coupled gradient HSQC experiments and by the S3CT pulse sequence of Sorensen and co-workers (*20*−*22*). To maximize the spectral resolution, three sets of t_1-folded experiments were acquired with spectral widths of 4000 Hz in the indirect dimension, one with the ^{13}C carrier position in the center of the anomeric region (∼95 ppm), another in the center of the ring region (∼70 ppm), and the last one in the methyl region (∼20 ppm).

For residual dipolar coupling measurements, a 15% bicelle stock solution in molar ratio 3:1 of 1,2-di-*O*-tridecanyl-*sn*-glycero-3-phosphocholine (13:0 diether PC) and 1,2-di-*O*-hexyl-*sn*-glycero-3-phosphocholine (6:0 diether PC) in D_2O was prepared. Lipids were purchased from Avanti Polar Lipids, Inc. This bicelle medium was chosen because of its improved chemical stability with respect to conventional phospholipid bicelles. The solution was mixed with vortexing in several cycles of heating to 40 °C and cooling on ice.

Molecular modeling was used as a tool for analysis, principally as a source of model structures to interpret dipolar couplings as is explained below. The model structures were generated using Macromodel Version 7 in 10000 cycles of Monte Carlo (MC) steps with the Amber force field. The GB/SA continuum solvent model implemented in Macromodel was used to represent water as solvent. This protocol has been reported as a suitable one in reproducing experimental dipolar coupling in oligosaccharides (*23*, *24*). In addition, a stochastic MD simulation with the same force field was carried out, also with Macromodel 7.0. The protocol included energy minimization of the initial structure and assignment of velocities corresponding to 300 K followed by equilibration for 1 ps. During 20 ns of MD simulation, random variations were introduced in the glycosidic dihedral angles accompanied by equilibration at 300 K. Glycosidic dihedral angles are defined following the IUPAC recommended heavy atom-based convention.

Dipolar coupling data were interpreted by calculating the optimal orientation tensor giving the best fit to the experimental C−H one-bond coupling values for each molecular model. The fitting algorithm, which uses Powell optimization, has been previously described by Azurmendi et al. (*23*). The quality of the fit was reflected in the merit function, χ, which measures the discrepancy between the experimental data and the values calculated for each molecular model. The definition, given in ref *24*, is the square root of the function, similar to that used in a number of other RDC studies. This approach was used for analysis of those domains of the hexasaccharide which are proposed to adopt a single rigid conformer. Since the full hexasaccharide is proposed to also contain some flexible domains, some additional calculations were carried out using the TRAMITE algorithm in which the orientation tensor of the entire oligosaccharide is calculated from the moment of inertia tensor of the molecular model (*25*).

RESULTS

For our preliminary studies, western blots were used to assay digestion. In our gel protocol, intact O139 CPS runs

near the top of the gel close to a 125 kDa protein marker. Gels from samples incubated with increasing amounts of phages in the range 10^2-10^{10} PFU showed a decrease in the intensity of staining associated with intact capsules and the appearance of ladders of bands in the region of 30−40 kDa protein markers. This result indicates digestion into discrete numbers of repeating subunits of the O139 capsule. This interpretation was confirmed by ^{1}H NMR spectra of the products of digestion with 10^9 PFU phages, which showed spectra similar to those of the parent polysaccharide but with greatly decreased ^{1}H NMR line widths and with NMR lines appearing at 5.73 and 5.90 ppm which are not seen in the polymer.

These results are consistent with reports by Linnerborg et al. (*14*) that treatment of *V. cholerae* O139 polysaccharide with this phage results in depolymerization by a phage-associated lyase which cleaves the bond between the GlcNAc residue and the GalA residue by β-elimination. (See Figure 1 for the structure of the product.)

To find optimum conditions for digestion of the polysaccharide, we incubated 0.6 mg of CPS under various conditions using UV absorbance at 232 nm to assay the extent of digestion. UV absorbance at this wavelength is characteristic of the $\Delta^{4,5}$-uronic acid which results from the β-elimination reaction, and this assay has been widely used for the various polysaccharide lyases which are commonly used for digestion of glycosaminoglycans.

In our experiments, we sought the maximum absorbance at 232 nm as an indication of maximum digestion of the polysaccharide. In experiments at fixed salt, pH, and CPS concentration, the amounts of phage were varied, showing some digestion with 10^4-10^6 PFU but with much more at 10^9-10^{10} PFU, consistent with our interpretation of the gels described above. With fixed phage at 10^{10} PFU, activity was observed to be low at pH 5, 6, or 8, with optimal activity at pH 7.0−7.5. The influence of Ca^{2+} was tested at pH 7. Addition of 5 mM $CaCl_2$ caused a small increase over control PBS, and 5 mM EDTA caused a small decrease which was not considered to be significant.

The products of a batch digestion of the polysaccharide were desalted and applied to a Bio-Gel P-6 column monitored by UV absorbance. The chromatograms showed an excluded peak and an included peak, both of which were collected and analyzed by NMR spectroscopy. The included peak had an NMR spectrum which was essentially identical to that reported by Linnerborg et al. (*14*), which is interpreted as that of the single hexasaccharide repeating unit of the O139 CPS as shown in the structure of Figure 1. The enzymatic activity of the phage is analogous to that of a number of microbial polysaccharide lyases which act on substrates containing 4-substituted uronic acids (*26*). These enzymes catalyze a β-elimination reaction, similar to that of chemical catalysis by base, breaking the polysaccharide chain and producing a 4,5-unsaturated sugar with characteristic UV absorption at 232 nm (*27*). The mechanism of polysaccharide lyases specific for a wide range of uronic acid containing polysaccharides has been studied, and a number of crystal structures have been recently reported (*28*). Since β-elimination leads to an unsaturated product planar at C4 and C5, galacturonate, glucuronate, and iduronate produce products of identical structure.

Table 1: NOE Data for the Hexasaccharide

proton pair[a]	NOE[b]	distance[d] (Å)	average distance md1[e]	average distance md2[f]
d-H1−e-H2	S	2.35	2.39	2.38
d-H1−e-H3	A	3.97	3.67	3.68
f-H1−b-H4	S	2.40	2.47	2.41
e-H1−b-H3	S	2.41	2.54	2.50
e-H2−f-H6	M	3.17[c]	3.34	3.36
b-H2−d-H5	W	3.33	2.78	2.92
c-H1−a-H4	M			
c-H1−a-H3	A			
a-H1−b-H6	W			
a-H1−b-H6′	A			

[a] Only the first six proton pairs were used in the calculations of the conformation of the tetrasaccharide epitope. [b] S = strong, M = medium, W = weak, and A = absent. [c] Distance e-H2−f-C6. [d] Distances in the best fit NOE model, 179. [e] MD trajectory 12.6−14.5 ns. [f] MD trajectory 15.9−18.2 ns.

The oligosaccharde fraction appearing in the excluded volume peak showed NMR lines at 5.73 and 5.90 ppm which are characteristic of the nonreducing terminal $\Delta^{4,5}$-uronic acid and also peaks at 5.41 ppm characteristic of internal galacturonic acid residue, implying that this is the dodecasaccharide or a mixture with higher oligosaccharides. [See Preston et al. (*16*) for NMR assignments of the intact polysaccharide.]

Fractions corresponding to the hexasaccharide were pooled and 2D NMR spectra were recorded on this sample. Analysis of the COSY, TOCSY, and HMQC spectra gave results largely consistent with the assignment reported by Linnerborg et al. (*14*) with the single exception that we find the ^{1}H resonance of residue d-H5 to be at 4.27 ppm. (See Figure 1 for the letters indicating residue assignments used in this paper.) Figure S-1 in the Supporting Information gives an NMR spectrum and Table S-1 chemical shift assignments for the hexasaccharide sample used for these experiments along with a review of other chemical data characterizing the products of lyase digestion. NOESY spectra of the hexasaccharide at room temperature and mixing times of 50, 200, and 800 ms all gave rather weak cross-peaks as expected for an oligosaccharide of this size. Therefore, spectra were recorded at 15 °C with mixing times of 150 and 300 ms, which showed substantial negative NOE cross-peaks. ROESY spectra, with 300 ms mixing time at room temperature and with the carrier outside the region of oligosaccharide resonances, showed cross-peaks similar to those of the low-temperature NOESY spectra except for the region near the HDO signal (4.73 ppm) which was obscured. A similar room temperature ROESY spectrum with the carrier on the water resonance allowed for convenient suppression of the interference from the HDO signal but showed some evidence of Hartmann−Hahn effects on a few of the cross-peaks. Analysis of the three spectra indicated consistency of the cross-peaks among the three spectra, and a qualitative summary of the cross-peak strengths of the three spectra is given in Table 1.

The dilute liquid crystal medium used for the measurement of residual dipolar coupling did not cause any significant change in the ^{1}H or ^{13}C chemical shifts of the hexasaccharide, implying that the bicelle medium does not specifically interact with the oligosaccharide. We will present below a discussion of the mechanism of orientation which is con-

Table 2: Residual Dipolar Coupling Data for the Hexasaccharide

proton	carbon	$^1D_{CH}$(exptl)[a]	model 179[b]	model 128[c]
a-H1	a-C1	6.0		
a-H4	a-C4	11.0		
a-H5	a-C5	7.5		
b-H1	b-C1	3.5	5.19	4.00
b-H3	b-C3	3.7	5.24	3.38
b-H4	b-C4	4.5	5.00	5.18
b-H5	b-C5	5.5	4.75	5.19
b-CN[d]	b-MN	7.7	6.97	6.53
c-H1	c-C1	1.7		
c-H2	c-C2	−6.7		
c-H3	c-C3	−2.0		
c-H4	c-C4	2.0		
d-H1	d-C1	1.8	2.95	0.43
d-H4	d-C4	0.4	−1.14	−1.25
d-H5	d-C5	11.0	5.26	9.49
d-M6[e]	d-C5	4.4	7.96	6.40
e-H1	e-C1	3.0	5.03	4.18
e-H2	e-C2	3.1	4.76	3.94
e-H3	e-C3	1.8	3.31	2.47
e-H4	e-C4	−11.4	−9.59	−9.86
e-H5	e-C5	2.8	5.42	4.57
f-H1	f-C1	−9.9	−10.96	−9.09
f-H4	f-C4	−10.8	−8.52	−7.95
f-H5	f-C5	3.1	−0.34	0.88
f-M6[e]	f-C5	−2.4	−5.57	−5.51

[a] Experimental error estimated to be ±1 Hz. [b] Calculated for tetrasaccharide model with lowest NOE error score, $\chi_{RDC} = 2.29$. [c] Calculated for tetrasaccharide model with best RDC fit to full tetrasaccharide RDC data having positive Ψ_{de},Ψ_{fb} and low *E*. $\chi_{RDC} = 1.147$. [d] Amide methyl group. [e] Colitose C6 methyl group.

sistent with a lack of strong binding interaction. One-bond C−H residual dipolar coupling data were measured by two NMR methods. In both, $^1J_{CH}$ were measured from splittings in spectra at 19 °C corresponding to the isotropic phase. Dipolar couplings were determined from the difference in $^1J_{CH}$ and splittings representing $J + D$ observed in 35 °C spectra corresponding to the oriented phase. In one series of experiments, gradient HSQC spectra were recorded with decoupling in the acquisition dimension and ^{1}H coupling in the indirect dimension. Another series of experiments utilized the S3CT method in which splittings were determined in the detected dimension from two separately recorded 2D spectra (*20*−*22*). Since the spectra in this latter method have only half as many peaks, spectral overlap is less troublesome and more peaks can be resolved. Therefore, most of the RDC data in Table 2 were taken from the S3CT data with an estimated error of ±1 Hz. The HSQC peaks for the methyl group resonances were well resolved and provided those RDC values. For a few peaks, those of a-H4, a-H5, and b-H5, small proton chemical shift differences could have given rise to homonuclear strong coupling interfering with the reliability of the S3CT data. It is clear from the assignments given in Table S-1 in the Supporting Information that those signals are all well resolved in the ^{13}C dimension so RDC data for those peaks were taken from HSQC spectra.

In the Monte Carlo simulation of the hexasaccharide, 10000 trials were sampled from which 3348 conformations having energy less than 50 kJ above the global minimum were kept for analysis. The models were sorted in order of increasing energy with model 1, the global minimum, set to 0 kJ/mol. On the basis of earlier studies (*11*), we have hypothesized that the tetrasaccharide epitope composed of residues **b**, **d**, **e**, and **f** in Figure 1 adopts a single rigid conformation. This tetrasaccharide has structural homology to the human blood group Lewis[b] epitope which has been extensively studied and shown to adopt a single conformer (*8*). Therefore, the residual dipolar coupling data were interpreted by finding an orientation of the tetrasaccharide epitope which optimizes the fit of the calculated and experimental data. RDC from methyl groups were interpreted with the direction of the C−C bond scaled by the ratio of the C−H to C−C bond length (*24*, *29*). The method used, which has been described previously, uses a Powell optimization in combination with certain measures to rapidly determine the best orientation tensor to describe the data (*23*, *24*). Since at least five independent vectors are required to calculate the orientation tensor by this method, one-bond ^{13}C−^{1}H dipolar coupling data are not adequate to orient each sugar ring independently, but for a rigid epitope in which several pyranoside rings tumble as a unit, this approach has been successful (*8*).

Two-dimensional maps were prepared in which either the calculated energy or the discrepancy between the experimental RDC and that calculated for the best orientation is plotted as a function of the dihedral angles of each of the glycosidic linkages in the tetrasaccharide. Figure 2 shows a plot for the Galβ-(1→3)-GlcNAc linkage (**e**−**b**) in which the discrepancy, χ_{RDC}, is plotted on a 5° grid. The energy map, Figure 2a, shows two regions of energy minima with the lower one near $\Phi_{e-b} = -75°$ and $\Psi_{e-b} = -100°$. This region also shows the best agreement with the dipolar coupling data (Figure 2c). For the linkages of the α-colitose residues, **d**−**e** and **f**−**b**, the lowest energy conformers (Figures 3a and 4a) are those with $\Phi = -70°$ and $\Psi = 135°$, but good fits to the RDC data are also found for conformers having dihedral angles in the region of −70°, −70° in Figures 3c and 4c. Most of these conformers have relatively high conformational energy of 30−40 kJ/mol above the global minimum.

The NOE data were reconciled with the molecular models according to the following algorithm. Proton pairs assigned strong NOE were assumed to be spaced at 2.4 Å, those assigned medium NOE at 2.8 Å, and those with weak NOE at 3.1 Å. The proton pair for which NOE was absent was assumed to be spaced at least 3.5 Å. For the spacing between e-H2 and the methyl group, f-H6, a distance between e-H2 and the methyl group carbon atom, f-C6, was taken to be 3.1 Å. Squared deviations for all the pairs indicated in the NOE data of Table 1 were summed to assign an NOE score for each model. This NOE score, χ_{NOE}, is also plotted for each of the three linkages in Figures 2b, 3b, and 4b. For the Galβ-(1→3)-GlcNAc linkage, **e**−**b**, minima in the NOE score, χ_{NOE}, are found only near the energy minimum at −75°, −100°. For the linkages of the α-colitose residues, good agreement with the NOE data is found only near the low-energy minimum at −70°, 135° and not near the secondary minimum seen for the RDC data near −70°, −70°. It is our interpretation that the agreement of the RDC data with these latter conformations is an artifact resulting from an inadequate amount of RDC data. We assume that with additional data these conformations could be rejected. Although the data of Figures 3 and 4 could be interpreted as indicating a virtual conformation, the NOE data argue against this possibility. All of the observed NOE peaks for the tetrasaccharide epitope can be explained by the proposed

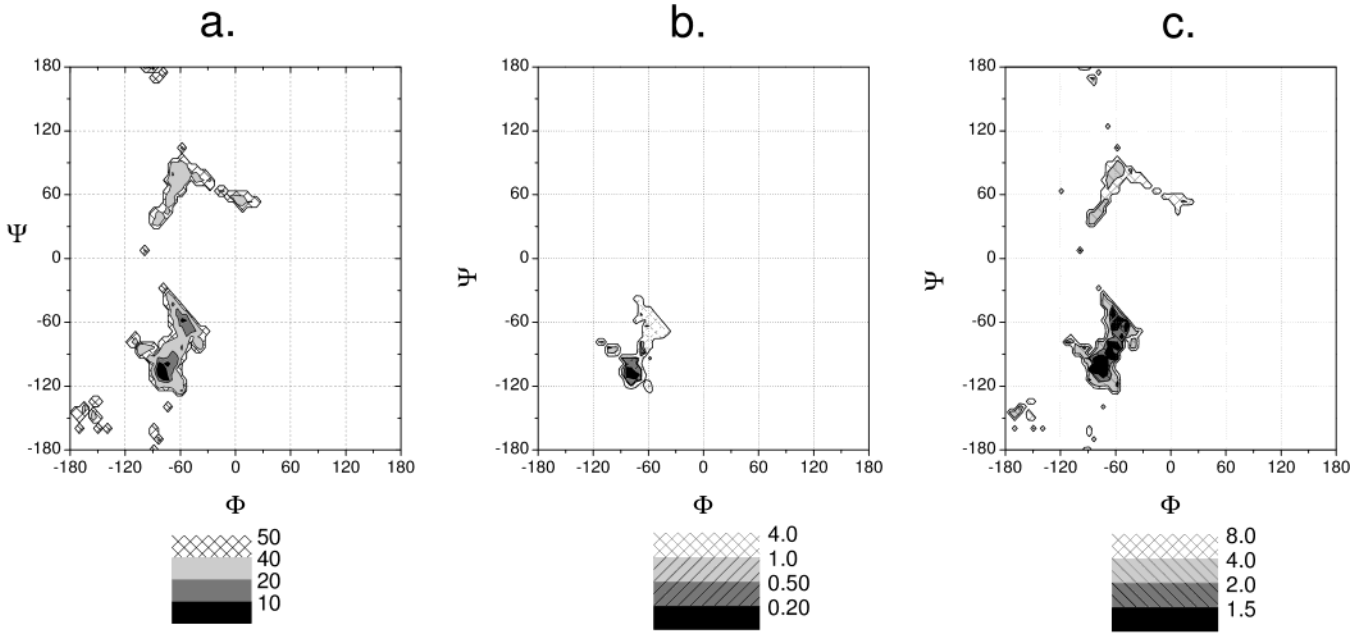

FIGURE 2: Contour plots from the Monte Carlo calculation describing dependence on the Gal β-(1→4)-GlcNAc linkage: (a) energy in kJ; (b) χ_{NOE}; (c) χ_{RDC}.

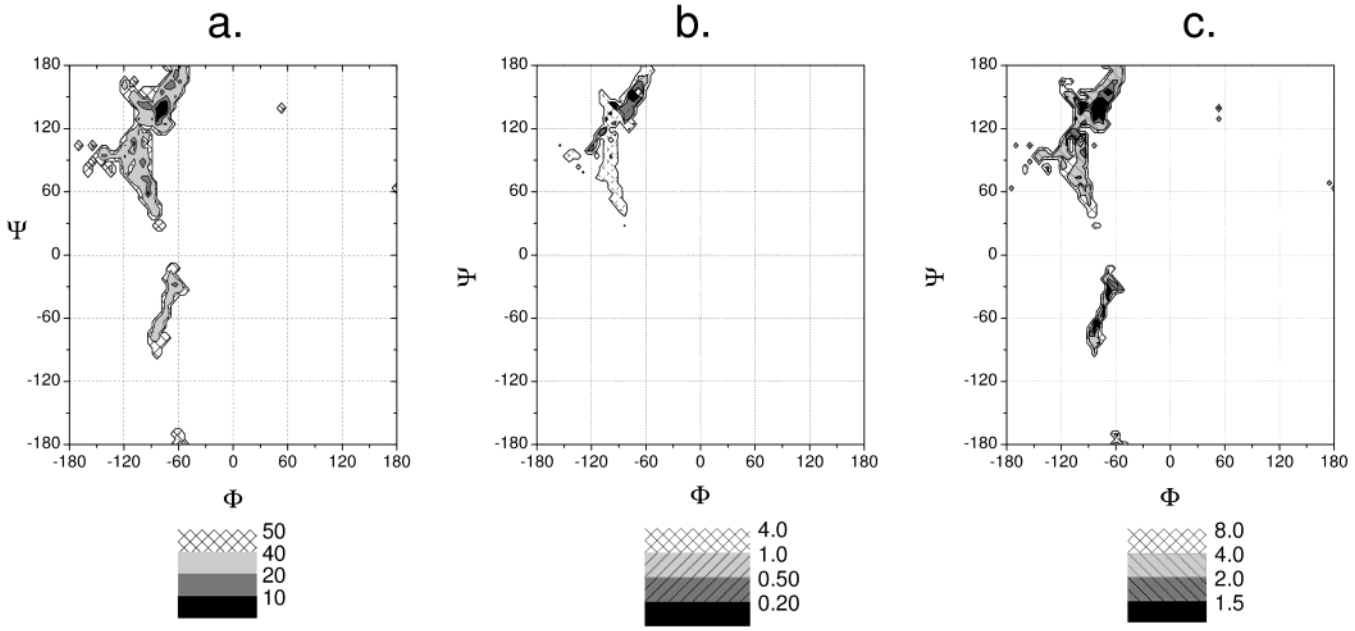

FIGURE 3: Contour plots from the Monte Carlo calculation describing dependence on the Col α-(1→2)-Gal linkage: (a) energy in kJ; (b) χ_{NOE}; (c) χ_{RDC}.

conformation, and since the method of interpretation accounts for absent cross-peaks, there are none expected on the basis of this conformation which are not observed. We will give only a qualitative interpretation of cross-peaks for residues **a** and **c** since flexibility complicates interpretation of NOE as will be discussed below.

Following this interpretation, we propose in Table 3 models for the tetrasaccharide epitope based on energy minima (first column, model 1), on best fit to the NOE data (second column, model 128 at 16.0 kJ/mol), and on best fit to the RDC (third column, model 179 at 18.6 kJ/mol). In selecting the conformation of the third column, we have rejected conformations with high energy and that have negative values of Ψ_{d-e} and Ψ_{f-b} which disagree with the NOE data. In Table 2, we present the RDC data calculated for each of these proposed models. That for the model (128) giving best fit to the experimental RDC data shows generally good agreement compared to the estimated experimental error for most of the RDC and discrepancies of about 2 Hz for the worst cases. The 2 Hz discrepancy is slightly greater than our estimated experimental error of ±1 Hz. While it is possible that we have underestimated the experimental error, such discrepancies have been noted in RDC studies on other epitopes thought to be rigid, and we believe it more likely to result from effects of fluctuations envisioned for internal motion of the first kind. It is our interpretation that the differences of 10−15° in Φ and Ψ among the different models of Table 3 represent a realistic estimate of dihedral

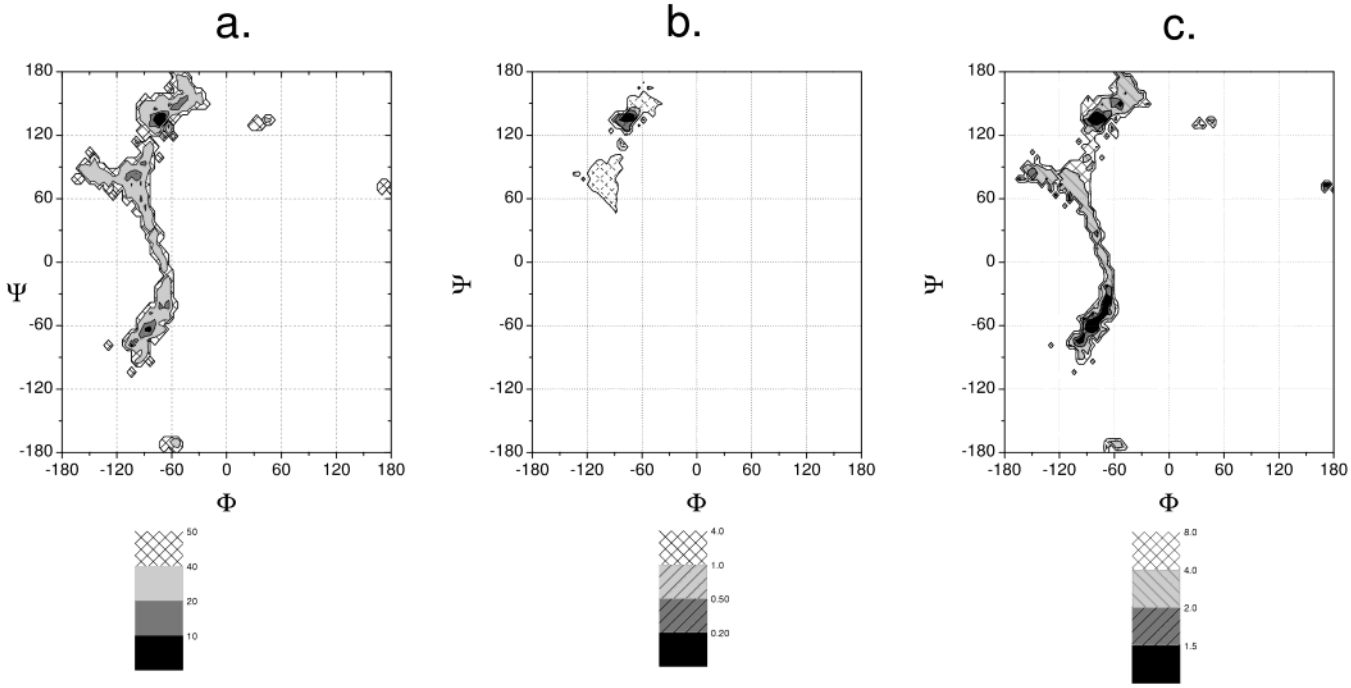

FIGURE 4: Contour plots from the Monte Carlo calculation describing dependence on the Col α-(1→4)-GlcNAc linkage: (a) energy in kJ; (b) χ_{NOE}; (c) χ_{RDC}.

Table 3: Proposed Models for the Tetrasaccharide Epitope

	lowest energy	best fit		MD average		
		NOE[a]	RDC[b]	12.6−14.5 ns	15.9−18.2 ns	M1[c]
energy (kJ)	0.0	18.6	16.0			
Φ_{d-e}	−73	−71	−69	−80	−82	−99
Ψ_{d-e}	137	122	135	139	139	125
Φ_{e-b}	−76	−77	−77	−72	−70	−66
Ψ_{e-b}	−103	−104	−93	−99	−102	−103
Φ_{f-b}	−70	−72	−74	−71	−73	−57
Ψ_{f-b}	136	139	135	138	138	143
χ_{NOE}	0.48	0.06	0.71	0.56	0.58	
χ_{RDC}	1.72	2.29	1.15	2.05	2.13	
model[d]	1	179	128			

[a] Model with lowest NOE error score. [b] Best fit RDC for models with positive Ψ_{de},Ψ_{fb} and $E < 20$ kJ. [c] Proposed model in the polysaccharide; Gunawardena et al. (*11*). [d] Models in the Monte Carlo calculation were sorted in order of increasing energy with model 1 the global minimum.

angle fluctuations for epitopes of the Lewis type, and RDC is very sensitive to small changes in angles.

To control for the possibility that the Monte Carlo calculation could introduce a bias in the molecular modeling leading to inadequate sampling of candidate conformations, a stochastic molecular dynamics calculation was also used as a source of conformers. In this method, random forces are applied periodically to displace glycosidic torsion angles in order to improve the extent of sampling of the conformational space. The resulting MD trajectory was analyzed to find conformations agreeing with the RDC and NOE data of Tables 1 and 2. Two-dimensional maps (not shown) of the NOE score, defined above, were prepared for all three linkages, with results similar to those of the NOE maps for the Monte Carlo calculation (Figures 2b, 3b, and 4b). All of the conformations found in the MD trajectory agreeing with the NOE data are in the same regions as indicated in column

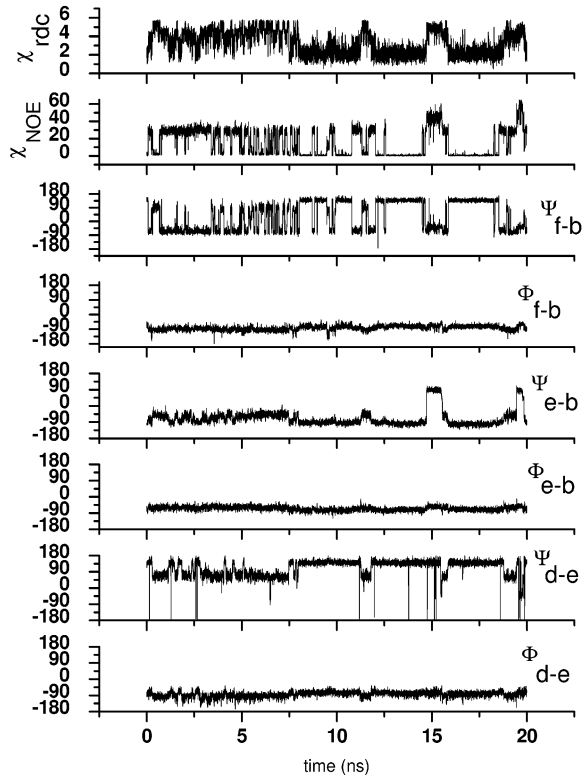

FIGURE 5: Stochastic MD trajectory of the hexasaccharide showing the history of the glycosidic dihedral angles of the tetrasaccharide epitope along with the NOE and RDC merit functions.

3 of Table 3. Figure 5 shows a trajectory plot of the dihedral angles of the tetrasaccharide along with the NOE score, χ_{NOE}, and the error function, χ_{RDC}, for the tetrasaccharide RDC data. The trajectory does not in any sense represent the true dynamics of the system since the stochastic forces heat the system which is then reequilibrated at 300 K. But the trajectory visits many conformations, most of which give

poor agreement with the NOE and RDC data. In the region of 12.6−14.5 ns and 15.9−18.2 ns, data calculated from the models agree well with the experimental data. Average values over these two regions were calculated for the distances involved in the NOE data and are included in Table 1. The distances are in good agreement with the NOE data, and the average NOE error function is also low as indicated in Table 3 and Figure 5. The average values of the RDC error function are also low in these parts of the trajectory. The average values of the glycosidic dihedral angles are very similar to those for the optimal models derived from the MC calculation and given in Table 3.

The conformational analysis represented in Tables 1−3 and in Figures 2−5 describes the tetrasaccharide epitope composed of residues **b**, **d**, **e**, and **f** under the assumption that it adopts a single relatively rigid conformation. In fact, all of the molecular modeling calculations, both Monte Carlo and molecular dynamics, include the complete hexasaccharide of Figure 1. The linkages of residues **c**−**a** and **a**−**b** are ignored in this analysis. We have no evidence that these two residues tumble as a rigid unit with the other four residues, and in fact, we hypothesize that the linkages **c**−**a** and especially **a**−**b** contribute significantly to the flexibility of the O139 capsular polysaccharide. That there must be some flexibility in the polysaccharide is indicated by the observation of reasonable line widths (≃5 Hz) in the NMR spectra of the intact capsule (*11*, *16*).

Since Tables 1 and 2 contain NOE and RDC data relevant to the conformation of the **c**−**a** and **a**−**b** linkages, those residues could be included in the analysis. We have carried out an analysis of the RDC data for the full hexasaccharide under the assumption that it can be represented by a single conformer. Plots of the RDC error function, χ_{RDC}, for the three linkages of the tetrasaccharide epitope (data not shown) are very similar to those in Figures 2c, 3c, and 4c, indicating that whatever flexibility exists in the **c**−**a** and **a**−**b** linkages does not seriously compromise the calculation of the orientation tensor. But plots of the energy and of the RDC error function, χ_{RDC}, for the **c**−**a** and **a**−**b** linkages are not consistent with single conformers, implying that an analysis accounting for multiple conformations for these two residues is required. We will discuss the prospects for such an analysis below.

Both energy calculations, Monte Carlo and molecular dynamics, indicate that the **c**−**a** linkage has somewhat limited flexibility with $\Phi_{c-a} \simeq 50°$ and $\Psi_{c-a} \simeq -150$ or $+60°$, with the former value of Ψ_{c-a} having the lower energy in the Monte Carlo calculations. In these lower energy conformations, the distance c-H1−a-H4 is greater than that between c-H1−a-H3, which is not consistent with NOE data of Table 1. Our MC calculation includes conformations with c−H1 closer to a-H4 than to a-H3, but they occur at higher energy. This observation could be explained by the fact that residue **c** is a $\Delta^{4,5}$-galacturonic acid, which may not be accurately described by the Amber force field used in our calculations. The requirement for a coplanar arrangment of C3, C4, C5, and the ring oxygen distorts the pyranoside ring into half-chair conformers rather than the normal chairs observed for common sugars, including all of the other pyranosides in the hexasaccharide (*30*). While the conformation of these unsaturated sugars has not been intensively studied, they are thought to be found in an equilibrium between two half-chairs, $^2H_1$ and $^1H_2$, the relative populations of which are controlled by electrostatic interactions with adjacent residues (*31*). Without a more reliable set of molecular modeling parameters for the half-chairs of residue **c**, it is difficult to verify the correctness of the conformation we have used, and it is possible that the conformation of the **c**−**a** linkage is not well represented in these calculations.

For the QuiNAc β-(1→6)-GlcNAc linkage, **a**−**b**, our energy calculations show multiple minima with two values of Φ and three values each for Ψ and ω, suggesting substantial flexibility for this linkage. While the interpretation of RDC data for relatively rigid oligosaccharide epitopes is straightforward, the description of a flexible structure requires statistical weights for all contributing conformers. The one-bond $^1H-^{13}C$ RDC data are adequate to define the orientation of the tetrasaccharide (**b**, **e**, **d**, and **f**), but more data would be required to describe the flexibility in the hinge region linking residues **c**−**a**−**b**. Of two approaches to interpreting RDC in flexible oligosaccharides, one involves treating each pyranoside ring as rigid and calculating orientation tensors for each ring separately. This method, which requires at least five independent vectors per residue, has been used to detect flexibility in oligosaccharides (*32*). A second method uses a collection of model conformers, from an MC or MD calculation, employing the proposed "steric shape-induced anisotropy" model of Zweckstetter and Bax (*33*) to calculate the orientation tensor for each model. From these data, RDC can be calculated for each model, and a simple ensemble average can be compared with experimental RDC (*34*, *35*). We have recently proposed a simple method (TRAMITE), based on these ideas, for calculation of the orientation tensor of a molecular model from its moment of inertia tensor and have tested the idea on a series of rigid oligosaccharides having known conformations (*24*, *25*). A preliminary analysis of the data of Table 2 with the TRAMITE method gives reasonable results which do not differ greatly from those illustrated in Figures 2−4. This analysis assumes a single conformation for the complete hexasaccharide. By including additional conformations in an average, we can obtain improved agreement with the experimental RDC data (data not shown). But it is clear that Table 2 has an insufficient number of independent RDC data to orient individual sugar residues, and it is likely that substantially more than five RDC vectors per residue might be needed to derive statistical weights for multiple conformers. Thus, without $^1H-^1H$ and two-bond $^{13}C-^1H$ RDC data and without a more realistic description of the unsaturated sugar, **c**, we consider it premature to attempt a critical evaluation of exactly which conformations for the **c**−**a** and **a**−**b** linkages should ideally be included in the average.

Our interpretation could be compromised by changes in the conformation of the hexasaccharide caused by strong binding interactions with the bicelles. The interactions responsible for orienting proteins and oligosaccharides have been extensively considered in the literature, and although some proteins may exhibit hydrophobic binding to lipid bicelles, this effect seems less likely for the more polar oligosaccharides. For the experiments described here, the degree of orientation is small (less than 10^{-3}), so the energy of interaction must be small compared to kT. For the case of electrically neutral bicelle media, this weak interaction is best described by the steric shape-induced alignment model

of Zweckstetter and Bax (*33*). This model has been extensively tested for proteins and is generally found to be valid in the absence of electrostatic effects (*25*, *33*, *36*, *37*). This model has also been applied successfully to oligosaccharides (*24*, *25*, *34*, *38*). It is our interpretation that this weak interaction mechanism is responsible for the orientation observed for the *V. cholerae* O139 hexasaccharide.

CONCLUSIONS

The use of residual dipolar coupling for oligosaccharides weakly oriented in liquid crystalline solutions is a relatively new method for studying their conformation, but the method shows great promise as an additional tool to supplement NOE which has been the major source of information on oligosaccharide conformation in solution. The method has been tested on several oligosaccharides whose conformations are relatively well understood, including the Lewis oligosaccharides (*8*, *23*), blood group A and B (*24*), and the trimannoside core of N-glycans (*32*, *35*) as well as sucrose (*39*) and other oligosaccharides (*38*, *40*). While NOE methods have been very successful for determining conformations of relatively rigid oligosaccharides, the results with highly flexible ones have been less clear. In principle, the complications in NOE analysis due to the dynamics of internal motion and overall tumbling should be less troublesome in the analysis of RDC, and eventually analysis for flexible oligosaccharides should be straightforward. Due to the novelty of the method, techniques for analysis are still under development. Analysis of RDC data, of the type used in this paper, is not thought to be correct for high molecular weight polysaccharides whose size is large compared to the bicelles of the orienting medium.

In a previous publication, we have described a conformation for the tetrasaccharide epitope of *V. cholerae* O139 in the intact polysaccharide on the basis of 3D NOE data on a ^{13}C-enriched sample (*11*). The molecular modeling methods differed in that study, and the 3D ^{13}C resolved NOE data gave more useful cross-peaks than we report here for the hexasaccharide. The glycosidic dihedral angles for the favored model, M1, from that study are compared in Table 3 with the models for the present study on the isolated hexasaccharide. The uncertainty in the dihedral angles in this study is about 10°, which is typical for oligosaccharides with internal motion of the first kind. Therefore, model M1 for the epitope in the polysaccharide is only slightly outside this range, consistent with the conclusion that the conformations of the epitopes are very similar in the polymer and the hexasaccharide and very similar to that of the Lewis^b blood group epitope.

Therefore, the *V. cholerae* O139 polysaccharide is not an example of the "conformational epitope" which has been discussed by Jennings and co-workers. This group has presented convincing evidence that the immunological response to a polysaccharide can depend on the number of repeating subunits as a result of conformational change with increasing size. For the case of meningococcal type B polysaccharides, strong immunological response is observed only for a chain length of about 10 residues or more, and evidence is presented for differences in the conformation of smaller oligosaccharides (*12*). They have also argued for a similar effect in group B streptococcal type III polysaccharides (*13*) as well as the pneumococcal type 14 polysaccharide (*41*). The physical evidence reported here for the absence of this effect in the *V. cholerae* O139 capsule is consistent with the observation of immunological cross-reactions with the LPS which contains a single copy of the hexasaccharide repeat of the polysaccharide (*3*).

ACKNOWLEDGMENT

Thanks are due to Dr. M. J. Albert for the gift of the bacteriophage JA-1 and to Dr. Alexander Sulakvelidze for helpful discussions.

SUPPORTING INFORMATION AVAILABLE

Figure S-1 showing the 500 MHz ^{1}H NMR spectrum of the hexasaccharide at room temperature and Table S-1 giving assignment data for the hexasaccharide at 27 °C. This material is available free of charge via the Internet at http://pubs.acs.org.

REFERENCES

1. Morris, J. G., Jr. (1994) *Vibrio cholerae* O139 Bengal, in *Vibrio cholerae and Cholera. Molecular to Global Perspectives* (Wachsmuth, I. K., Blake, P. A., and Olsvik, O., Eds.) pp 103−116, ASM Press, Washington, DC.
2. Albert, M. J. (1996) *Indian J. Med. Res. 104*, 14−27.
3. Waldor, M. K., Colwell, R., and Mekalanos, J. J. (1994) *Proc. Natl. Acad. Sci. U.S.A. 91*, 11388−11392.
4. Cox, A. D., Brisson, J. R., Varma, V., and Perry, M. B. (1996) *Carbohydr. Res. 290*, 43−58.
5. Breg, J., Romijn, D., Vliegenthart, J. F. G., Strecker, G., and Montreuil, J. (1988) *Carbohydr. Res. 183*, 19−34.
6. Cagas, P., and Bush, C. A. (1990) *Biopolymers 30*, 1123−1138.
7. Mukhopadhyay, C., and Bush, C. A. (1991) *Biopolymers 31*, 1737−1746.
8. Martin-Pastor, M., and Bush, C. A. (2000) *Biochemistry 39*, 4674−4683.
9. Delbaere, L. T., Vandonselaar, M., Prasad, L., Quail, J. W., Wilson, K. S., and Dauter, Z. (1993) *J. Mol. Biol. 230*, 950−965.
10. Bush, C. A. (2002) Origins of flexibility in Complex Polysaccharides, in *NMR Spectroscopy of Polymers in Solution and the Solid State* (Cheng, H. N., and English, A. D., Eds.) ACS Symposium Series, Vol. 834, pp 272−288, Oxford University Press, New York.
11. Gunawardena, S., Fiore, C. R., Johnson, J. A., and Bush, C. A. (1999) *Biochemistry 38*, 12062−12071.
12. Evans, S. V., Sigurskjold, B. W., Jennings, H. J., Brisson, J. R., To, R., Tse, W. C., Altman, E., Frosch, M., Weisgerber, C., Kratzin, H. D., Klebert, S., Vaesen, M., Bitter-Suermann, D., Rose, D. R., Young, N. M., and Bundle, D. R. (1995) *Biochemistry 34*, 6737−6744.
13. Brisson, J. R., Uhrinova, S., Woods, R. J., van der Zwan, M., Jarrell, H. C., Paoletti, L. C., Kasper, D. L., and Jennings, H. J. (1997) *Biochemistry 36*, 3278−3292.
14. Linnerborg, M., Weintraub, A., Albert, M. J., and Widmalm, G (2001) *Carbohydr. Res. 333*, 263−269.
15. Morris, J. G., Jr., Losonsky, G. E., Johnson, J. A., Tacket, C. O., Nataro, J. P., Panigrahi, P., and Levin, M. M. (1995) *J. Infect. Dis. 171*, 903−908.
16. Preston, L. M., Xu, Q., Johnson, J. A., Joseph, A., Maneval, D. R., Husain, K., Reddy, G. P., Bush, C. A., and Morris, J. G. (1995) *J. Bacteriol. 177*, 835−838.
17. Albert, M. J., Bhuiyan, N. A., Rahman, A., Ghosh, A. N., Hultenby, K., Weintraub, A., Nahar, S., Kibriya, A. K., Ansaruzzaman, M., and Shimada, T. (1996) *J. Clin. Microbiol. 34*, 1843−1845.
18. Sambrook, J., Fritsch, E. F., and Maniatis, T. (1989) *Molecular Cloning, A Laboratory Manual*, 2nd ed., Cold Spring Harbor Laboratory Press, Cold Spring Harbor, NY.
19. Comstock, L. E., Johnson, J. A., Michalski, J. M., Morris, J. G., Jr., and Kaper, J. B. (1996) *Mol. Microbiol. 19*, 815−826.

20. Meissner, A., Duus, J. O., and Sorensen, O. W. (1997) *J. Biomol. NMR 10*, 89−94.
21. Sorensen, M. D., Meissner, A., and Sorensen, O. W. (1997) *J. Biomol. NMR.10*, 181−186.
22. Lerche, M. H., Meissner, A., Poulsen, F. M., and Sorensen, O. W. (1999) *J. Magn. Reson. 140*, 259−263.
23. Azurmendi, H. F., Martin-Pastor, M., and Bush, C. A. (2002) *Biopolymers 63*, 89−98.
24. Azurmendi, H. F., and Bush, C. A. (2002) *Carbohydr. Res. 337*, 905−915.
25. Azurmendi, H. F., and Bush, C. A. (2002) *J. Am. Chem. Soc. 124*, 2426−2427.
26. Sutherland, I. W. (1995) *FEMS Microbiol. Rev. 16*, 323−347.
27. Kiss, J. (1974) *Adv. Carbohydr. Chem. Biochem. 29*, 229−303.
28. Jedrzejas, M. J. (2000) *Crit. Rev. Biochem. 35*, 221−251.
29. Ottiger, M., Delaglio, F., Marquardt, J. L., Tjandra, N., and Bax, A. (1998) *J. Magn. Reson. 134*, 365−369.
30. Jansson, P. E., Lindberg, B., Manca, M. C., Nimmich, W., and Widmalm, G. (1994) *Carbohydr. Res. 261*, 111−118.
31. Ragazzi, M., Ferro, D. R., Provasoli, A., Pumilia, P., Cassinari, A., Torri, G., Guerrini, B., Casu, B., Nader, H. B., and Dietrich, C. P. (1993) *J. Carbohydr. Chem. 12*, 523−535.
32. Tian, F., Al-Hashimi, H. M., Craighead, J. L., and Prestegard, J. H. (2001) *J. Am. Chem. Soc. 123*, 485−492.
33. Zweckstetter, M., and Bax, A. (2000) *J. Am. Chem. Soc. 122*, 3791−3792.
34. Almond, A., Bunkenborg, J., Franch, T., Gotfredsen, C. H., and Duus, J. O. (2001) *J. Am. Chem. Soc. 123*, 4792−4802.
35. Almond, A., and Duus, J. O. (2001) *J. Biomol. NMR 20*, 351−363.
36. Fernandez, M. X., Bernardo, P., Pons, M., Garcia, J., and Garcia de la Torre, J. (2001) *J. Am. Chem. Soc. 123*, 12037−12047.
37. Almond, A., and Axelsen, J. B. (2002) *J. Am. Chem. Soc. 124*, 9986−9987.
38. Lycknert, K., Maliniak, A., and Widmalm, G. (2001) *J. Phys. Chem. A 105*, 5119−5122.
39. Neubauer, H., Meiler, J., Peti, W., and Griesinger, C. (2001) *Helv. Chim. Acta 84*, 243−258.
40. Landersjo, C., Hoog, C., Maliniak, A., and Widmalm, G. (2000) *J. Phys. Chem. B 104*, 5618−5624.
41. Laferriere, C. A., Sood, R. K., De Muys, J.-M., Michon, F., and Jennings, H. J. (1998) *Infect. Immun. 66*, 2441−2446.

BI026700T